

TRITIUM INVENTORY CONTROL

TASK: Studies on tritium permeation into various materials as a function of gas composition, partial pressure and temperature

*S. Brad, I. Stefanescu, L. Stefan, A. Lazar, M. Vijulie, N. Sofilca, A. Bornea, F. Vasut,
M. Zamfirache, N. Bidica,*

National Institute for Cryogenics and Isotopes Technologies, Rm. Valcea,

C. Postolache, L. Matei

“Horia Hulubei” National Institute of Physics and Nuclear Engineering, Bucharest

As a result of the high probability of hydrogen isotopes permeation through materials during high-temperature reactor operation, the interaction of hydrogen isotopes with metallic structural materials proposed to be used for fusion reactor designing, is of a great importance for safety considerations. Determining the parameters of the interaction between heavy hydrogen isotopes and various materials, including diffusion, solubility and permeation of tritium through structural materials, is therefore essential to accurately calculate recycling, out gassing, loading, permeation and hydrogen embrittlement. The permeation tests were made at “Horia Hulubei” National Institute of Physics and Nuclear Engineering Bucharest for radioactive protection reasons, inside of a special glove-box, at different tritium concentration values.

1. Study of Hydrogen isotopes permeation into various materials as a function of gas composition, partial pressure and temperature

1.a Experimental details

The experimental stand was built in order to perform tests with different materials and with different concentrations of tritium. In Figure 1 is shown the experimental device. The experiments were performed at different concentrations of tritium in HT gas. The variation of the concentration of tritium and of course of the partial pressures was done in a decreasing mode by adding hydrogen gas, in the hydrogen/tritium supply vessel. The program of investigation is shown in the Table 1. The volume of HT gas for each sample was 140 mL with a total concentration 585, 43 $\mu\text{Ci/mL}$. The time period for each test was set at 100 h, and after that the permeated product was burned to water in a catalyst burner. The volume of tritiated water measured by a Liquid Scintillation Counter (LSC) was 3.5 ml. All the samples

were protected in order to not have a contact with air because even small amounts of oxygen at the surface can change the permeation rate. Oxide layers at the surface are usually used for to reduce protium, deuterium or tritium permeation. Also the permeation of hydrogen through metals is influenced by trapping at internal defects.

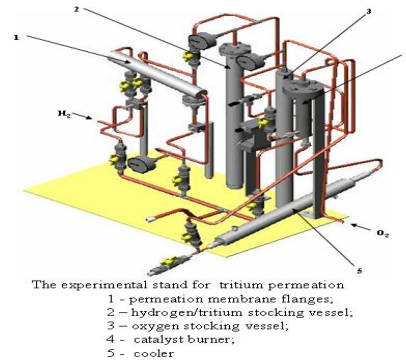


Figure 1 – Experimental stand for hydrogen isotopes permeation

In case of metals, the fundamental permeation equation [1-3] can be written as

$$\frac{dQ}{dt} = P \frac{A}{d} (\sqrt{p_u} - \sqrt{p_d})$$

where $\frac{dQ}{dt}$ is the number of H/D/T moles permeated per second through a sample of area A and thickness d, p_u (p_d) is the pressure of hydrogen on the upstream (downstream) side of the sample and P the permeability. Therefore for different concentration, temperatures and partial pressure we have

$$P = \frac{dQ}{dt} \frac{d}{A} \frac{1}{(\sqrt{p_{u,H,D,T}} - \sqrt{p_{d,H,D,T}})}$$

For metals we have also a relation which expresses the permeability:

$$P = P_0 \exp(-E_p/kT);$$

$$P = P_0 T \exp(-E_p/kT)$$

where P_0 is a pre-exponential factor, E_p the activation energy for permeation and k the Boltzmann constant. Permeability can also be described as the product of solubility and diffusivity.

Table 1- Investigation parameters

Sample	Thickness (mm)	Temperature (K)	Pressure before the membrane (Pa)	Total activity(on the burned water) (Bq)
Al 99.99%	0.25	500K	1.9×10^5	425.912
Al 99.99%	0.13	500K	1.9×10^5	486.817
Al 99.99%	0.13	500K	2.2×10^5	498.124
Al 99.99%	0.13	550K	1.9×10^5	521.567

The permeation rate was calculated and the value of these is between $4.2 \div 5.6 \times 10^{-5}$ (mol/msPa^{1/2}) for the aluminium membrane. The superior value of this range was achieved in condition of higher temperature and pressure. In all the experiments the samples were materials with high purity and the tests were performed without any contact with atmosphere or other impurities for metals. For the aluminium membrane we investigate the possibility of Hydrides formation. Analysis performed with a diffractometer system using the Powder Diffraction File database, did not reveal any Al-H bonds, as could be seen in the diffraction spectra given in Figure 2.

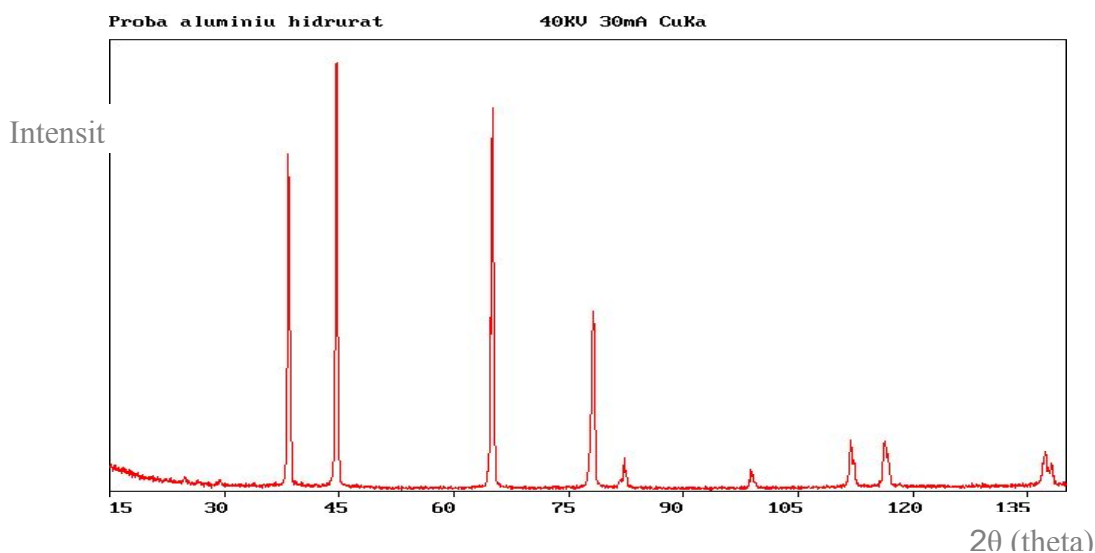


Figure 2 – X-ray diffraction spectra for Al 99.99% (0.25mm)

The aluminium membrane (used in permeation tests) spectrum is the same as the spectrum of a normal aluminium sample. In a rare case, hydrogen forms with aluminium to form hydrides of type Al-H₃. A Permeation, test was also made for tungsten at 1100K at 2.3×10^5 Pa and the permeation rate calculated was $P = 7.2 \times 10^{-7}$ mol/msPa^{1/2} and for nickel membrane at 500K and 2.0×10^5 Pa the permeation rate was $P = 3.1 \times 10^{-7}$ mol/msPa^{1/2}

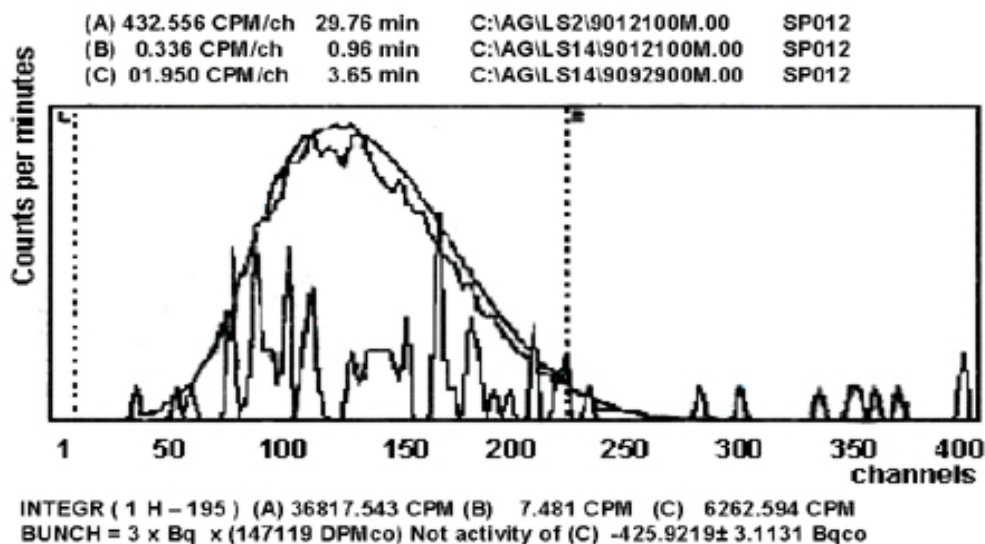


Figure 3 – Liquid scintillation spectra for Al 99.99% (0.25mm)

1.b Test stand modification by the elimination of the cryostat used for cooling , design for the sample specific polystyrene foam like a thermal protection envelope and the cryogenic liquid , make tension test at a specialized laboratory.

For the influence of helium, hydrogen and deuterium on different materials two different types of stainless steel described in the following table, were chosen:

Table 2 – Values of allied elements of the investigated stainless steels

Type	C %	Si %	Mn %	P %	S %	Cr %	Mo %	Ni %
W1.4006 (X10Cr13)	0,08-0,12	1	1	0,045	0,03	12-14	-	-
W1.4404 (X2CrNiMo 18 10)	≤0,03	1	2	0,045	0,03	16,5-18,5	2-2,5	11,0-14,0

For each stainless steel we have a programme of investigation in order to determine the influence of corrosion factors, helium and hydrogen isotopes and internal defects, on the properties of materials at different temperatures. The samples were cooled down at -200°C and broken in order to observe the influence on the toughness. With X-Ray Diffraction (XRD) analysis the concentration of the Fe α % and Fe γ % were determined. The other phases were produced by a corrosion treatment in diluted solution of HCl (18.3%) or HNO₃ (27.7%). All these metallic phases produced by different treatments, decrease strongly the toughness of the steels, with values in the range 10-30%.

For two samples of W1.4006, a surface mechanical treatment (work hardening) was applied in order to modify the dislocation concentration. The work hardening of a crystalline material is a complex phenomenon, because the stress necessary to move a dislocation depends both on short-range interactions such as the intersection of forest dislocations, and long-range interactions with both near and distant dislocations. Despite a considerable research effort in this area, a complete understanding of the subject has

not yet been achieved, even for single crystals. The problem has two parts. First, the variation of dislocation content with strain must be determined. Second, the dependence of the flow stress on the dislocation content must be determined. For this sample an increase of the toughness and mechanical resistance was observed, in correlation with the increased value of the dislocation concentration (dislocations induced by the rolling mechanical process applied to the samples).

Table 3 - Temperature of investigation, treatments mode and impact energy values

Material	Temp (K)	Energy (J)
W1.4006(not treated sample)	300	112
W1.4006(not treated sample)	73	92
W1.4006 (treated sample in acid)	73	80
W1.4006 (treated sample in hydrogen)	73	85
W1.4006 (treated sample in helium)	73	90
W1.4006 (work hardening)	73	95
W1.4404(not treated sample)	300	145
W1.4404(not treated sample)	73	102
W1.4404(treated sample in acid)	73	99
W1.4404(treated sample in hydrogen)	73	97
W1.4404(treated sample in helium)	73	98

1.c X-Ray Diffraction (XRD) measurements

Data acquisition was made with a DRON UM1 diffractometer connected to a PC. A horizontal powder goniometer in Bragg-Brentano geometry with graphite monochromator was used. The incident Cu-K α radiation, $\lambda = 1.54178 \text{ \AA}$ was used. The typical experimental conditions were: 2 sec. for each step, range angle $2\theta = 10^0-100^0$, step 0.05^0 . The spectra obtained in these conditions were used to make qualitative and quantitative phase analysis and to determine the microstructure parameters by *pattern fitting method* [4-6].

Table 4 – Sample description for stainless steel W1.4006

Type	Code	Sample description and preparation method
W1.4006	4006_eta	Etalon: Cr (12-141)%, Si (1%), Mn (1%), S (0.03%), P (0.045%), C (0.08-0.12)%, Fe
W1.4006	W1_4006	W1.4006/HCl/30min./470 ⁰ C /1h
W1.4006	W1_4006a	W1.4006/.../790-820 ⁰ C /30min/HCl
W1.4006	W1_4006b	W1.4006/He/740-820 ⁰ C /30min/HNO3
W1.4006	W_4006c	W1.4006/HNO3
W1.4006	W_4006b	W1.4006/He/750-820 ⁰ C /30min.

Table 5 – Sample description for stainless steel W1.4404

Type	Code	Sample description and preparation method
W1.4404	4404_eta	Etalon: Cr (12.5-18.5%), Ni (11-14%), Mo (2-2.5%), Si (1%), Mn (2%), S (0.03%), P (0.045%), C under 0.03%, Fe
W1.4404	W1_4404	W1.4404/He/1050 ⁰ C/1h
W1.4404	W1_4404a	W1.4404/H2/30 min/500 ⁰ C /HNO3
W1.4404	W1_4404b	W1.4404/HCl/12 h/H2/30min/470 ⁰ C
W1.4404	W1_4404c	W1.4404/1050 ⁰ C /5-10 min/He/470 ⁰ C

Qualitative phase analysis on W1.4006 and W1.4404 of the presence of Fe α (martensite) and Fe γ (austenite) is presented in Table 6. The estimated concentrations are provided by analysis of the figures and of the diffraction patterns (Figs.4&5).

Table 6 – Qualitative phase analysis on W1.4006 and W1.4404

Samples W1.4006	Concentrations estimated of Fe α % and Fe γ %	Samples W1.4404	Concentrations estimated of Fe α % and Fe γ %
4006_eta	0% and 100%	4404_eta	100% and 0%
W1_4006	<1% and >99%	W1_4404	<10% and >90%
W1_4006a	~50% and ~50%	W1_4404a	<1% and >99%
W1_4006b	<10% and >90%	W1_4404b	~100% and ~0%
W_4006c	~100% and ~0%	W1_4404c	>99% and <1%
W_4006b	~100% and ~0%		

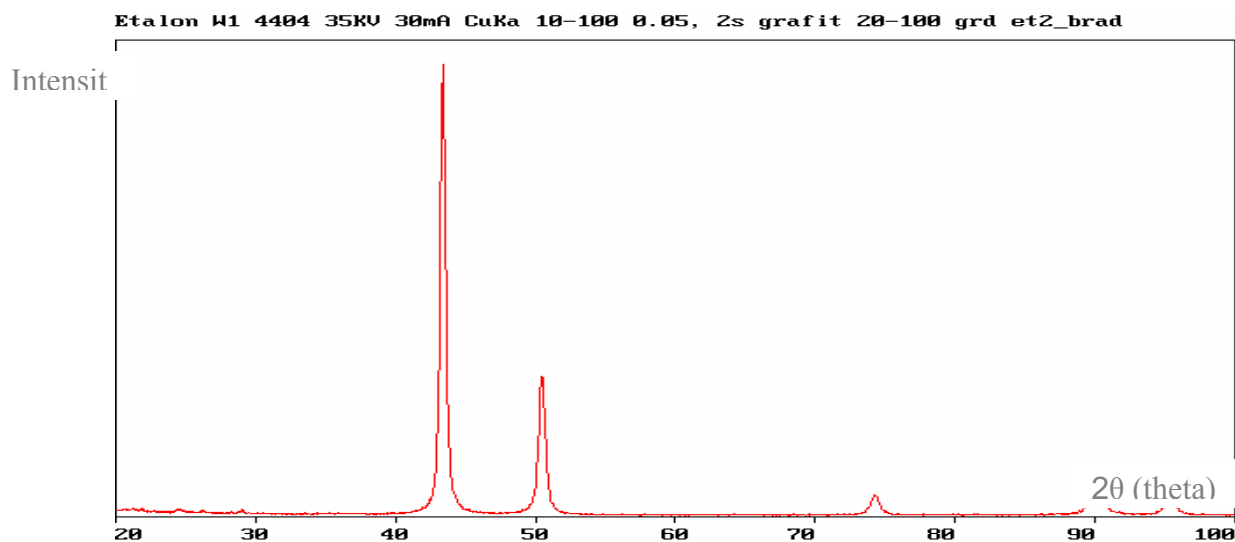


Figure 4 - Etalon X-Ray diffraction spectra for W1.4404

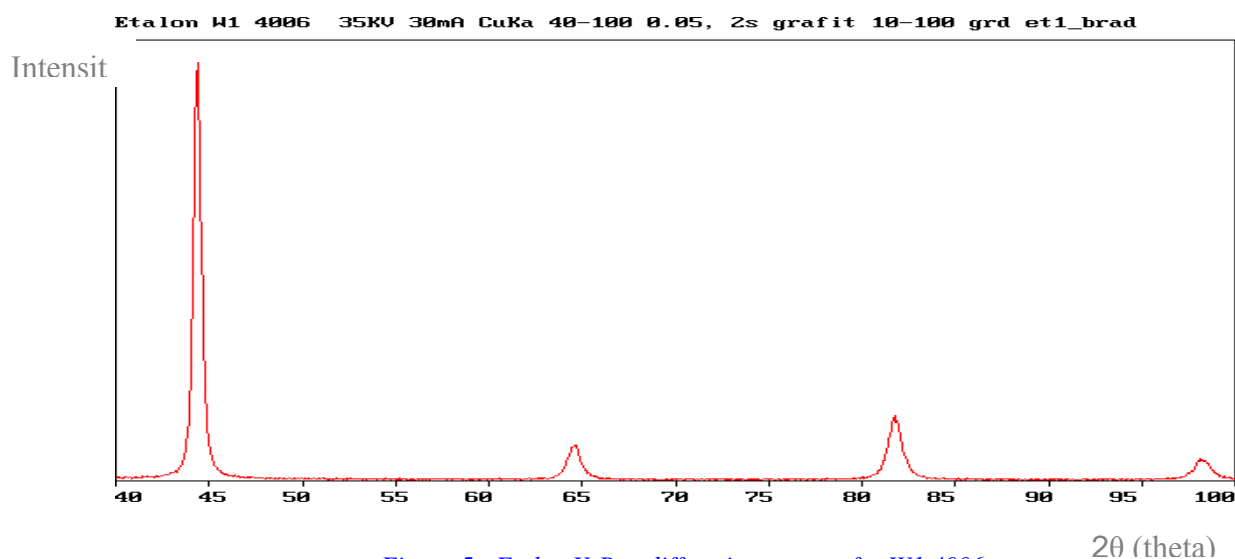


Figure 5 - Etalon X-Ray diffraction spectra for W1.4006

For W1.4404, treated in hydrogen atmosphere, the scanning electron micrograph of the fracture surface is shown in Figure 6.

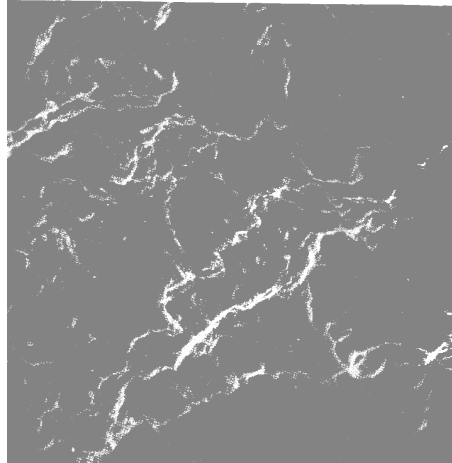


Figure 6 – Scanning electron micrograph sample (W1.4404)

It can be seen the many nuclear cavities from which ridges emanate. The morphology of internal voids and cracks, in hydrogen embrittled steels, leaves little doubt that growth commonly occurs by the development of new surface progressively at the roots of notches because broad expanses of relatively smooth surface are exposed. Fracture studies using the scanning electron microscopy seem to place the sites of cavity nucleation too far apart in relation to the height of the ridges of final rupture, as can be seen in the Figure 6. Fracture has followed grain boundaries.

The mechanical proprieties of the materials decrease for the samples treated in corrosive hydrogen, helium atmosphere (Table 3). Hydrogen and deuterium can influence the behavior of materials significantly. A facile explanation of hydrogen embrittlement is a reduction in the parameters of the Orowan-Irwin-Griffith equation so as to lower the critical stress for brittle cleavage. If an external stress is applied to a polycrystalline structure, the dislocations will first move in a grain having a large critical resolved shear stress [7]. However, as dislocations cannot in general cross a grain boundary, they will pile up at the boundary until the stress there is sufficient to generate slip in an adjacent grain. At this point, general plastic flow can occur, and the material is said to have yielded. The role of the hydrogen and deuterium in fracture mechanism is that of a perturbation on the basic strength of the metals. Theoretically strength we can consider the maximum strength obtained for the laboratory defect-free metal whiskers. For industrial metals and also for small strains these systems approximate elastic behavior, but the bulk of the stress-strain curve is discussed in terms of glissade dislocations and their interactions. In dislocation theory, the perfect lattice is replaced by a structure less elastic continuum through which dislocation forges may be transmitted. This simplification is relaxed to allow the existence of point defects, such as vacancies or interstitial atoms which in turn may combine with each other to form compound defects, often referred to as complexes or with dislocations to form Cottrell atmospheres. With these components, the dislocation-dislocation repulsion, dislocation-dislocation coalescence, and dislocation-interstitial attraction can explain effects such as work-hardening, internal crack formation, yield point, internal friction.

For the samples with work hardening treatment, the subsequent deformation of the material, dislocation pile-ups will occur not only at grain boundaries, but at other obstacles formed during the deformation, e.g. glissade dislocations such as the type of the Lomer-Cottrell barrier in face-centered-cubic (FCC) materials [8-9]. Not only will such barriers force the generation of new dislocations, thus increasing the dislocation density, and hence the flow stress, but the dislocation pile-ups have a long-range stress field which affects the mobility of dislocations on other slip planes. Several work hardening theories based on the long-range stresses from dislocation pile-ups have been formulated. At a sufficiently large applied stresses, the barriers will either be overcome, or broken by the dislocations, and the rate of work hardening will be reduced.

Further, more small changes in the chemical composition, the grain size, the degree of plastic constraint caused by a notch or flaw, and even the rate at which a load is applied can all have a marked effect on the strength, toughness, and the temperature at which the ductile-to-brittle transformation occurs. In this way, another important factor is the mechanism of the movement and propagation of dislocation in the body-centered-cubic metals and alloys.

Conclusions

The permeation experiments show an increase of the tritium permeation rate at small increasing of temperature and pressure. Oxide layers at the surface are usually used to reduce protium, deuterium or tritium permeation. Also the permeation of hydrogen through metals is influenced by trapping at internal defects. Superior value of permeation rate will be achieved in conditions of higher temperature and pressure. In all the experiments, the samples were materials with high purity and the tests were performed without any contact with atmosphere or other impurities for metals. Also an important result is that for the aluminum we determine the impossibility of Hydrides formation.

For the influence of hydrogen, helium and internal defects, the use of body-centered-cubic metals at low temperatures have to be undertaken with considerable care, with the increasing of any other external or internal factors (stress, hydrogen corrosion, temperature, dislocations and other crystalline defects). An important reason for why we developed this study of the comportment and movements of the dislocations in a body-centered-cubic is that the ferritic and martensitic steels are cheaper than the austenitic steels. With the group of parameters tables and data compilations that we obtained with this study, we can lower the temperature at values where those steels may be employed safely. These works have relevance to JET and ITER facilities.

References:

- [1]. Forcey K.S., Ross D.K., Simpson J.C.B. and Evans D.S., J. Nucl. Mater. 160 (1988), 117.
- [2]. Serra E., Perujo A. and Benamati G., J. Nucl. Mater. 245 (1997), 108
- [3]. Serra E. and Perujo A., J. Nucl. Mater. 240 (1997), 215.

- [4]. **Warren B. E.**, 1969, X-Ray Diffraction, (Reading MA Addison-Wesley).
- [5]. **Warren B. E. and Averbach B.L.**, 1950, J. Appl. Phys. 21, 595.
- [6]. **Ducu C., Malinowski V., Iosub I.**, 2003, Rev. Chimie, 54, 8, 666.
- [7]. **Kaname Kizu, Alexander Pisarev and Tetsuo Tanabe**,
J. Nucl. Mater. 289 (2001), 291-302.
- [8]. **Tomofumi Shiraishi, Masabumi Nishikawa, Takahiro Yamaguchi and Kentaro Kenmotsu.**, J. Nucl. Mater. 273 (1999), 60-65.
- [9]. **A. A. Yukhimchuk' and V. K. Gaevoy**, J. Nucl. Mater. 233-237 (1996), 1193-1197.

Publications:

Brad S., Lazar A., Vijulie M., Gherghinescu S., “*Toughness stand modification by the elimination of the cryostat used for cooling, design for the sample specific polystyrene foam like a thermal protection envelope.*”, Cryogenics 2004, Praga.

Brad S., Vijulie M., Gherghinescu S., Dragoiu C., Lazar A., “*Helium in materials use in hydrogen cryogenic distillation.*”, ICATE 2004, Craiova, Romania.